RESEARCH ARTICLE
10.1002/2016JA022414

Key Points:
- Multiple regression can control for correlated predictors of relativistic electrons
- ULF wave activity and solar wind number density and velocity are best predictors
- Solar wind and IMF parameters affect flux through intermediate processes as well as directly

Correspondence to:
L. E. Simms,
simmsl@augsburg.edu

Empirical predictive models of daily relativistic electron flux at geostationary orbit: Multiple regression analysis

Laura E. Simms[1], Mark J. Engebretson[1], Viacheslav Pilipenko[2], Geoffrey D. Reeves[3], and Mark Clilverd[4]

[1]Augsburg College, Minneapolis, Minnesota, USA, [2]Institute of the Physics of the Earth, Moscow, Russia, [3]Los Alamos National Laboratory, Los Alamos, New Mexico, USA, [4]British Antarctic Survey, Cambridge, UK

Abstract The daily maximum relativistic electron flux at geostationary orbit can be predicted well with a set of daily averaged predictor variables including previous day's flux, seed electron flux, solar wind velocity and number density, AE index, IMF B_z, Dst, and ULF and VLF wave power. As predictor variables are intercorrelated, we used multiple regression analyses to determine which are the most predictive of flux when other variables are controlled. Empirical models produced from regressions of flux on measured predictors from 1 day previous were reasonably effective at predicting novel observations. Adding previous flux to the parameter set improves the prediction of the peak of the increases but delays its anticipation of an event. Previous day's solar wind number density and velocity, AE index, and ULF wave activity are the most significant explanatory variables; however, the AE index, measuring substorm processes, shows a negative correlation with flux when other parameters are controlled. This may be due to the triggering of electromagnetic ion cyclotron waves by substorms that cause electron precipitation. VLF waves show lower, but significant, influence. The combined effect of ULF and VLF waves shows a synergistic interaction, where each increases the influence of the other on flux enhancement. Correlations between observations and predictions for this 1 day lag model ranged from 0.71 to 0.89 (average: 0.78). A path analysis of correlations between predictors suggests that solar wind and IMF parameters affect flux through intermediate processes such as ring current (Dst), AE, and wave activity.

1. Introduction

Fluxes of energetic electrons (kinetic energy > 1.5 MeV) in Earth's outer radiation belts vary over several orders of magnitude. As high levels of energetic electrons can damage sensitive electronic components of satellites [*Baker et al.*, 1987, 1998a; *Lanzerotti*, 2001; *Pilipenko et al.*, 2006], an empirical model would be helpful in predicting these flux changes.

Correlations between flux enhancements and activity in the solar wind and magnetosphere have long been recognized [*Simms et al.*, 2014 and references therein]. Empirical predictive models using the association between flux and these parameters may best be constructed from a set of variables so as to model contributions from all factors. Several studies have analyzed contributions from more than 1 factor simultaneously, finding independent contributions from a combination of solar wind velocity and number density [*Lyatsky and Khazanov*, 2008; *Balikhin et al.*, 2011; *Kellerman and Shprits*, 2012], from a combination of velocity, pressure, geomagnetic indices, and flux on the previous day [*Ukhorskiy et al.*, 2004; *Sakaguchi et al.*, 2015], from velocity, IMF orientation, and Dst [*Li et al.*, 2011], from combined ultra low frequency (ULF) and very low frequency (VLF) wave activity [*O'Brien et al.*, 2003], or from ULF activity and storm levels of Dst [*O'Brien and McPherron*, 2003].

In the present study, we build on this empirical work by incorporating all these variables in a single analysis, as well as including a measure of substorm activity (the auroral electrojet index, or AE) and seed electron flux (100 keV). This allows the simultaneous test of several proposed and interlinked mechanisms for flux enhancement, including acceleration of electrons by ULF wave activity [*Elkington et al.*, 1999; *Green and Kivelson*, 2004; *Liu et al.*, 1999; *O'Brien et al.*, 2003] and VLF wave activity [*Horne and Thorne*, 1998; *Summers and Ma*, 2000a; *Albert et al.*, 2009; *Tu et al.*, 2014]. VLF wave activity may be increased by energy injected during substorms [*Kim et al.*, 2000, 2015; *Meredith et al.*, 2002; *O'Brien et al.*, 2003; *Rodger et al.*, 2016], and substorms may increase the population of seed electrons which may be accelerated to relativistic energies [*Baker et al.*, 1998b].

As many of these empirical predictors are correlated with each other [*Lyons et al.*, 2005; *Simms et al.*, 2010; *Potapov et al.*, 2012, 2014; *Borovsky and Denton*, 2014], only a few may correlate well with electron

enhancements when other variables are held constant. A set of intercorrelated predictors such as this can be studied with multiple regression analysis, which determines the relative importance of the predictors when others are held constant [*Neter et al.*, 1985; *Simms et al.*, 2010; *Golden et al.*, 2012].

Additionally, a factor that correlates well with electron enhancement may not be a direct driver of increased flux. Instead, it may influence electron flux indirectly through an intermediate factor. As an example, a model might be proposed where electrons are accelerated by ULF or VLF wave power, which are in turn excited by the energy provided by high-speed solar wind streams. Although the high velocity and number density of these streams may not directly increase electron acceleration, they would correlate well with a rise in flux because they are responsible for injecting energy into wave activity which is the direct driver. Correlations of possible predictors with electron enhancement would not distinguish between this proposed mechanism and a mechanism where solar wind parameters directly influence electron acceleration.

The relative influence of direct and indirect effects can be differentiated with the use of path analysis, which extends multiple regression to estimate the magnitude of causal connections between a set of variables [*Loehlin*, 1991]. In this study, we use this technique to shed light on which of the many predictors of relativistic electron flux can be said to directly drive enhancements and which are the indirect correlates.

2. Data and Methods

In our database of predictors covering 1992–2002 (1993 missing), there are approximately 3000 days for which we have a daily average of all variables and their lags on the three preceding days.

We obtained hourly averaged electron fluxes for relativistic electrons ($>$1.5 MeV) and seed electrons (100 keV) from several spacecraft (Los Alamos National Laboratory (LANL) energetic particle Synchronous Orbit Particle Analyzer (SOPA) instruments in geosynchronous orbit). No spacecraft was in operation for this entire period, so we averaged over all available satellites in each hour. As each satellite was calibrated differently, we first converted each hourly average to a standardized score with mean 0 and standard deviation of 1 by subtracting the overall mean for that satellite and dividing by the standard deviation of the satellite. For each day, we then found the maximum relativistic electron flux J_R and seed electron flux J_S of these average hourly values. We use the maximum to attempt to reduce the effect of diurnal variations in electron fluxes. We also note that the maximum J_R is of more interest than the average, as damage to satellites is most likely to occur during the highest fluxes.

As predictor variables beyond seed electron flux, we used measures of ULF (ultra low frequency) and VLF (very low frequency) wave power. We use a ground-based ULF index covering local times 0500–1500 in the Pc5 range (2–7 mHz) obtained from magnetometers stationed at $>\sim$ 45°N [*Kozyreva et al.*, 2007]. We use the 1.0 kHz VELOX (VLF/ELF Logger Experiment) channel of Halley VLF (power measurements in this channel include frequencies from 0.5 to 1.5 kHz), limited to the dawn period (9–12 UT, 6–9 MLT). This frequency range and time period are dominated by dawn chorus, the VLF category thought to have the most influence on relativistic electron flux [*Smith*, 1995; *Smith et al.*, 2004b]. In addition, we obtained AE, Kp, IMF B_z component, solar wind velocity (V_x in GSE coordinates), and number density (N) from the Omniweb data base. We found the daily average of these predictive variables. Unlike with the relativistic flux, the averages of these variables are of most interest as they more accurately describe the physical processes occurring in the magnetosphere. For the multiple regression analyses, all variables were converted to rankit normal scores [*Sokal and Rohlf*, 1995] by ranking each observation and then replacing its rank by the position, in standard deviation units, of the ranked items in a normally distributed sample of the same size. This transformation gives a normal distribution, which allows the use of statistical tests that depend on normality.

We performed cross correlations between J_R and the daily averages of the above parameters over all days in the study. However, due to high correlations between predictor variables, it is necessary to control for all other variables when determining the influence of each on flux [*Simms et al.*, 2014]. To correct for this problem, we report partial correlations in addition to the simple correlations. A partial correlation analyzes the association between two variables while holding all other variables constant.

We also performed a number of multiple regression analyses with J_R as the dependent variable. A multiple regression analysis can determine the relative influence of parameters on the dependent variable.
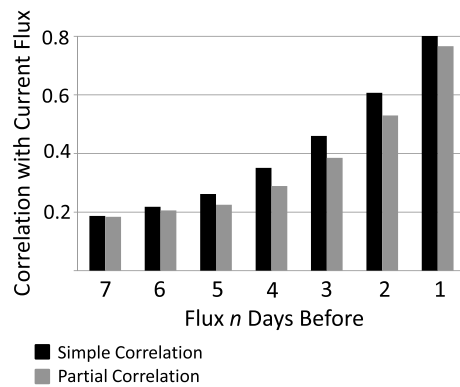
Figure 1. Correlation of relativistic electron flux with itself on preceding days. High simple correlations show flux is persistent over a number of days. Partial correlations (accounting for all other predictors) show somewhat less influence of the autocorrelation of flux when other variables are accounted for.

Mathematically, the predicted response variable (Y_i, the predicted J_R) is a linear combination of the prediction parameters (X_i) multiplied by their regression coefficients (b_i) for each of the i observations:

$$Y_i = b_0 + \Sigma b_i X_i \qquad (1)$$

We analyzed models with no lags in the predictor variables (a nowcast model), as well as with predictor variables from the previous 1 and 3 days. We also incorporated an interaction term between ULF and VLF wave activity. This variable is the product of each ULF and VLF observation. A significant effect of this variable in the regression model would indicate a synergistic effect where the action of one variable is enhanced by the other.

A lag term for J_R (the value of the flux on the previous day) was added to the models for several reasons. First, the persistence of these electrons means that flux levels are highly dependent on the levels the day before. Second, as the flux on a given day is highly dependent on the previous day's flux, this autocorrelation may decrease the error terms used in significance testing and lead to the conclusion that some predictor variables are important correlates when they are, in fact, not. The addition of previous day's flux corrects for this autocorrelation. (We do drop the lagged flux for one of the models used to assess prediction ability as we were not testing significance of the parameters).

We could have used change in flux as the dependent variable, but there was no advantage to this approach. Preliminary analyses showed that flux change was as highly correlated with previous day's flux as flux itself, as well as being highly correlated with the previous day's change in flux. Thus, this would have introduced another unnecessary covariate without any improvement in the clarity of the model.

Another method for dealing with autocorrelation in the dependent variable is two-stage regression in which a correction factor for the autocorrelation is introduced. The choice of which method to use (two-stage regression or simply the introduction of a lagged term) depends on the purpose of the model. If only a predictive "black box" model is desired, then two-stage regression may be a useful method. If, however, one desires to understand the physical processes and if one of those physical processes is, in fact, the persistence of the dependent variable, then it makes sense to use the method of adding a lagged term.

As the equations include at most one time lag, we suppose that the underlying state equation corresponds to a first order differential equation in time (e.g., a diffusion-like equation) rather than to a second order differential one (e.g., a wave equation).

We determined the best models by calculating R^2, the coefficient of determination. This statistic gives the fraction of variability in the data described by the model. In other words, it gives a measure of how well the model fits the data it is based on, although it says nothing about how well this model will predict new observations from outside the data set used to create the model. In simple linear regression, R^2 is equivalent to the square of the correlation coefficient, r. A coefficient of multiple correlation can be computed by taking the square root of R^2 and can be useful for rough comparisons of models. It should be noted that in linear multiple regression models, the R^2 statistic is mathematically equivalent to the prediction efficiency statistic used by *Turner et al.* [2011] and *Sakaguchi et al.* [2015]. However, neither the coefficient of determination (R^2) nor the prediction efficiency is a validation test. To validate our "best" models we correlated the observations from each year with predictions made by a model incorporating all other years. Each prediction was obtained by entering each observation's predictor parameters into the least squares regression equation.

In addition to the regression analyses with only J_R as the predicted variable, we set up a path diagram to study the correlational links between the independent variables [*Loehlin*, 1991; *Simms et al.*, 2010]. The dependent variable in each analysis is predicted by all the independent variables, but several of the independents may
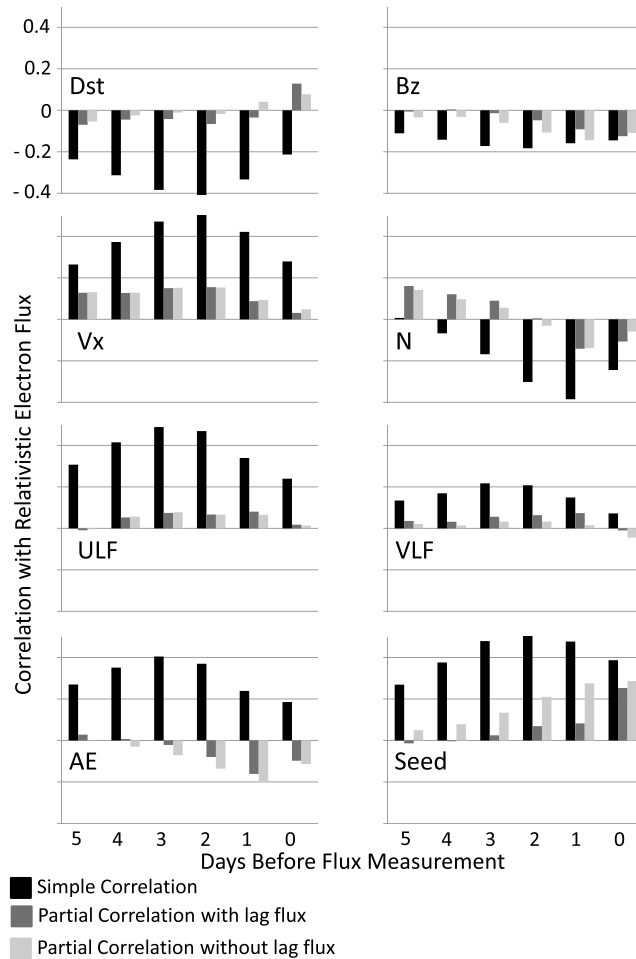
Figure 2. Cross correlation of flux with various parameters from day 0 (nowcast, measured on same day as dependent variable relativistic electron flux) to day 7. For most parameters, simple correlations (black bars) are higher than partial correlations for which other variables are held constant (gray bars). Partial correlations show the association of a parameter with flux when all other parameters are accounted for, including flux itself on prior days.

also be predicted by each other. Path analysis uses a series of multiple regressions with each predictor that could conceivably be influenced by the other predictors as dependent variable. In the diagram created from this, each path is given a weight representing the influence of one variable on another. These weights are the standardized regression coefficients from the multiple regression analyses. Thus, some independent variables may have both direct effects on the ultimate dependent variable as well as indirect effects by their influence on other independent variables. We used a prediction model with all independent variables measured 1 day before flux.

The unstandardized regression coefficients, together with measured predictor variables, can be used to forecast relativistic electron flux in new time periods. To test the ability of this method to predict new observations, we performed a series of multiple regressions, leaving each year out of the analysis in turn. We then predicted values for that year's data, using the measured values of the independent variables multiplied by the regression coefficients. We study three predictive models with this technique: a nowcast model and two 1 day lagged models. In the lagged models, all predictor variables are lagged; however, in one, the lagged flux (J_R) is added as a predictor while in the other it is not. Statistical analyses were performed in IBM SPSS Statistics and IDL (Interactive Data Language).
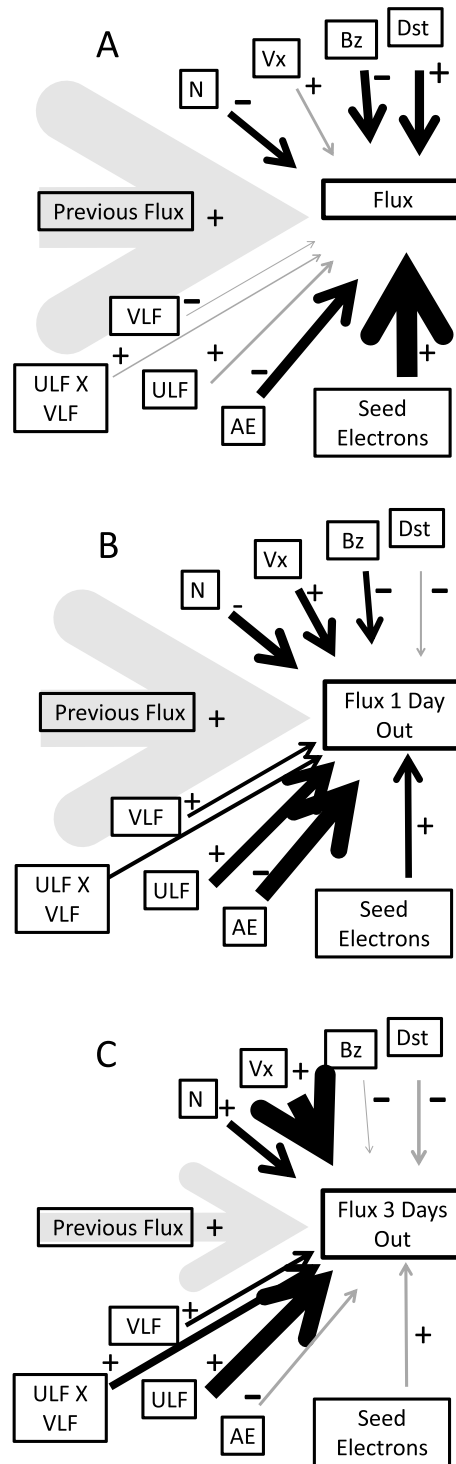
3. Results

Relativistic electrons are highly persistent in geosynchronous orbit, as can be seen by the flux autocorrelations (Figure 1; black bars: simple correlations; gray bars: partial correlations). Flux measured the day before shows a simple correlation of 0.806 with the current day's flux. The correlation 7 days earlier is still noticeable (0.187). When other predictors are accounted for in the partial correlations (gray bars), the correlation of flux with itself still ranges between 0.766 (previous day's flux) and 0.184 (flux 7 days earlier).

The highest correlations between other predictors and flux do not occur on the current day (Figure 2, day 0). The greatest simple correlations (black bars) occur 1 day (N), 2 days (B_z, Dst, V_x, and J_S), or 3 days (ground ULF and VLF, and AE) before the flux measurement. Using the same set of data, when other variables are held constant in partial correlation analysis, the correlations of predictor variables with flux are much lower (gray bars). This is largely due to the flux persistence. The previous day's flux can, by itself, accurately predict flux on most days. However, persistence cannot explain changes in flux that may occur abruptly. These must be due to other factors which should be incorporated into the model. Additionally, partial correlations calculated with

Figure 3. Influence of predictors on relativistic electron flux. A: Nowcast: Measurements for all variables are taken on the same day. B: Prediction: Predictors measured 1 day before relativistic electron flux. C: 3 day prediction: Predictors measured three days before. Statistically significant factors are represented by black arrows. However, previous flux, while always a significant factor, is represented with a gray arrow to avoid clutter and emphasize the effects of the other predictors. The sign of each regression coefficient is given in the figure. Standardized regression coefficients for this figure are in Table 1.

previous day's flux (dark gray bars) and without it (light gray bars) are similar for most of the predictors. Thus, previous day's flux is not the sole reason why other predictors lose their high simple correlation. Many of the predictors appear to act as mutual proxies for one another.

Of the predictors with strong simple correlations, only V_x, N, and J_S maintain partial correlations greater than 0.1. AE also retains a stronger partial correlation, but opposite in sign. To more accurately determine the relative influences, we use a series of regression analyses. A current day nowcast (with previous day's flux as a covariate to control for persistence) shows that same day, J_S is the most influential variable, followed (in order of influence) by AE $(-)$, Dst $(+)$, B_z $(-)$, and N $(-)$ (sign denotes positive or negative influence). The effects of V_x, ULF, VLF, and the ULF-VLF interaction are not significant when measured on the same day as J_R (Figure 3a). Arrow thicknesses represent the relative influence of parameters as measured by the standardized regression coefficients given in Table 1. Black arrows are statistically significant effects ($p < 0.05$). Gray arrows (except flux) represent nonsignificant effects. Flux, while always significant, is represented by gray so as to reduce clutter in the figures. The percent variation explained by the model (R^2) is 70.7%. This is roughly equivalent to the square of the correlation coefficient (≈ 0.84).

The prediction of flux by parameters from 1 day previous shows a strong negative influence of AE, followed by ULF $(+)$, N $(-)$, V_x $(+)$, J_S $(+)$, B_z $(-)$, VLF $(+)$, and the ULF-VLF interaction $(+)$ in order of influence (Figure 3b). The percent variation in the data explained by this prediction model is 72.1% (roughly equivalent to a correlation of 0.85). In contrast, the simple correlation of previous day's flux with flux the next day is 0.80 (Figure 1), meaning that previous flux alone explains only 64.0% percent of the variation in flux.

A model could be constructed using the most correlated lag of each predictor with flux as determined by the simple correlations. Instead of the 1 day lag model presented in Figure 3b, the regression

Table 1. Coefficients of the Regression Models of Figure 3[a]

	Nowcast (Figure 3a)	1 Day Lag Prediction (3B)	3 day Lag Prediction (3C)
Dst	0.111[b]	−0.025	−0.044
B_z	−0.105[b]	−0.075[b]	−0.014
V_x	0.035	0.101[b]	0.257[b]
N	−0.088[b]	−0.116[b]	0.100[b]
ULF	0.034	0.143[b]	0.205[b]
VLF	−0.004	0.051[b]	0.056[b]
ULF × VLF interaction	0.019	0.048[b]	.095[b]
AE	−0.126[b]	−0.207[b]	−0.037
Seed electron flux	0.253[b]	0.083[b]	0.035
Lag relativistic electron flux	0.746[b]	0.700[b]	0.354
R^2 (% variation explained)	70.7%	72.1%	40.5%

[a]The coefficient of determination (R^2) is the percent variation in the data explained by the model. It is roughly equivalent to the square of the correlation coefficient.
[b]Effect significant at $p < 0.05$.

would include a 1 day lag term for N; 2 day lag terms for Dst, V_x, IMF B_z, and J_S; and 3 day lag terms for ULF, VLF, and AE. These models are compared in Table 2. (For comparison purposes, the sample size was reduced to the 2325 days on which all these variables were available for these lags. Thus, the coefficients of the 1 day lag model in Table 2 are slightly different from that in Figure 3b.) Choosing lags based on the highest simple correlations gives a model with a lower R^2 (the percent variation in the data explained by the model). In addition, most variables with higher simple correlations at a 2 day lag (B_z, V_x, and J_S) or at a 3 day lag (ULF, VLF, and AE) show less influence in the mixed lag regression model than when the 1 day lag of all variables is used. This suggests that the higher simple correlations at longer lags are not meaningful in a physical sense.

When predictors are measured 3 days previous, V_x shows the strongest influence (+), followed by ULF (+), N (+), the ULF-VLF interaction (+), VLF (+), and Dst (−) (Figure 3c). The percent variation explained is much lower ($R^2 = 40.5\%$, roughly equivalent to a correlation of 0.67). The influence of V_x, N, and ULF and VLF wave activity are highest when measured 3 days before, while the influence of Dst, B_z, AE, and J_S drop off farther from the current day.

The surprising negative influence of AE in the multiple regression models led us to repeat these models without this factor (Table 3). This reduces the effect of ULF activity in the 1 day lag model but has little influence on the effect of ULF or VLF activity in either the nowcast or the 3 day lag model. The percent of variation explained by the nowcast, 1 day lag, and 3 day lag models without AE are 71.3%, 70.4%, and 40.5%, respectively. These are nearly the same percent variation for models with AE shown in Table 1.

Substorms are thought to increase relativistic electron flux by injecting seed electrons and/or increasing ULF waves which then act to increase relativistic electron flux. Therefore, the excitation of these two processes by substorms may completely explain the positive influence of AE as it acts solely as an indirect driver of flux.

Table 2. Coefficients of Regression Models With Varying Lags[a]

	All Variables at Lag 1[b]	Lags Chosen by Highest Simple Correlation[c]
Dst	−0.031	−0.058[d] (Lag 2)
B_z	−0.079[d]	−0.015 (Lag 2)
V_x	0.112[d]	0.062[d] (Lag 2)
N	−0.155[d]	−0.127[d] (Lag 1)
ULF	0.126[d]	0.037 (Lag 3)
VLF	0.043[d]	0.027[d] (Lag 3)
AE	−0.209[d]	−0.065[d] (Lag 3)
Seed electron flux	0.083[d]	0.069[d] (Lag 2)
Lag1 relativistic electron flux	0.700[d]	0.693[d] (Lag 1)
R^2 (% variation explained)	71.4%	69.6%

[a]$N = 2325$ days for both models.
[b]Lag 1 model for all variables.
[c]The lag for each predictor variable chosen by its highest simple correlation.
[d]Effect significant at $p < 0.05$.

Table 3. Coefficients of the Multiple Regression Models With *AE* Removed From Model

	Nowcast	1 Day Lag Prediction	3 Day Lag Prediction
Dst	0.104[a]	−0.039[a]	−0.047
B_z	−0.072[a]	−0.018	−0.004
V_x	0.025	0.080[a]	0.253[a]
N	−0.097[a]	−0.131[a]	0.098[a]
ULF	−0.050	0.009	0.182[a]
VLF	−0.008	0.041[a]	0.055[a]
ULF × VLF interaction	0.020	0.053[a]	0.096[a]
Seed electron flux	0.241[a]	0.056[a]	0.031
Lag relativistic electron flux	0.750[a]	0.712[a]	0.356[a]
R^2 (% variation explained)	70.4%	71.3%	40.5%

[a]Effect significant at $p < 0.05$.

We test this hypothesis by doing a regression with only *AE* and then adding ULF and seed electron flux. Using just the 1 day lag model, we reduced the parameters in the multiple regression to only *AE* and the previous relativistic electron flux as a covariate (Table 4). In this analysis, the *AE* still shows a positive influence. However, when either ULF wave activity or seed electron flux is added to this reduced model, *AE* has a negative effect. This supports the hypothesis that the positive influence of *AE* (as seen in the simple correlations) is only a measure of its indirect effect through either or both of increased ULF wave activity or injected seed electrons. (A similar analysis could be done with VLF waves, but the effect of ground VLF waves in our study was so small that we did not attempt it.)

3.1. Model With No Persistence: An Example of Path Analysis

The interactions between predictor variables can be explored with the use of path analysis. In this analytical technique, a causal relationship between variables is proposed where each predictor has a direct effect on the final dependent variable (relativistic electron flux, in this case) as well as possible indirect effects by virtue of their influence on other predictors. Multiple regression is used to assess the degree of influence of the other variables on each predictor, with each intermediate variable, in turn, being used as the dependent variable.

In our path model, we posit that solar wind parameters (velocity, density, and IMF B_z) may influence relativistic flux not only directly but, perhaps more importantly, also indirectly through processes measured by *Dst* and *AE*, J_S, and ULF and VLF wave power. The arrival of energy in the solar wind triggers a response in both the *Dst* and *AE* indices, which roughly represent ring current and substorm activity, respectively. Both these mechanisms have been proposed as intermediary processes that drive wave activity and seed electron enhancements. We represent them in our model as variables controlled by solar wind parameters on the one hand but driving wave activity and J_S on the other. Thus, the processes measured by *Dst* and *AE* have both direct and indirect influences on J_R. We have chosen to eliminate persistence in our path model so as to reduce the complexity. If flux persistence is dropped, the regression of J_R on the other 1 day lagged predictors explains 31.8% of the variation (roughly analogous to a correlation coefficient of 0.564). As a predictive model, this would appear to be less accurate than the 1 day lag model with persistence included; however, we discuss below why the model without persistence may be more useful in some ways.
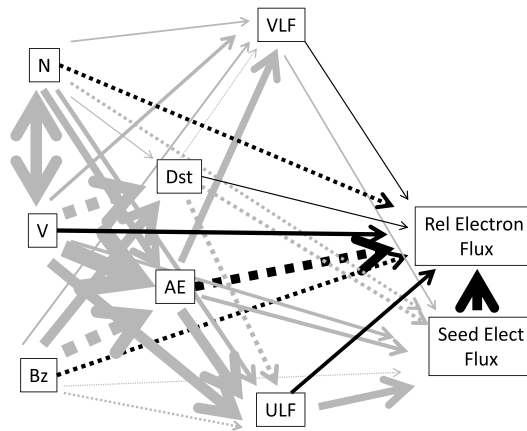
A test of this set of hypotheses is presented in Figure 4, where each arrow thickness represents the relative influence of predictors on J_R and on each other. Direct effects are represented by black arrows and intermediate effects by gray arrows. Dashed lines represent negative influences. All predictors are measured 1 day previous to flux.

Table 4. Regression Parameters From Multiple Regression, With Previous Relativistic Electron Flux as Covariate: *AE* Alone, *AE* With ULF, *AE* With Seed Electron Flux, and *AE* With Both ULF and Seed Electron Flux[a]

Previous Flux	*AE*	ULF	Seed Flux
0.789	0.096		
0.763	−0.177	0.315	
0.723	−0.072		0.251
0.722	−0.209	0.206	0.19

[a]While *AE* shows a positive influence on its own, the addition of either ULF or seed electron flux to the model causes the *AE* influence to become negative.

Predictors' direct effects are determined from the multiple regression where J_R is the dependent variable. The other path coefficients are from multiple regressions where each predictor is used as the dependent variable (Table 5). Not shown in Table 5 is the correlation between *N* and *V* of −0.529. The correlation between *N* and B_z (−0.002) and *V* and B_z (<0.001) were both negligible and

Figure 4. Path diagram of direct and indirect influences of predictors on relativistic electron flux. Each arrow thickness represents the relative influence of predictors on relativistic electron flux and on each other, with negative influences given by dashed lines. Direct effects are represented by black arrows and intermediate effects by gray arrows. The correlations between V and B_z, and N and B_z are essentially 0 and are therefore left out of the diagram.

therefore left out of the figure. Indirect effects are calculated as the sum of the product of all path coefficients from each predictor to J_R. Total effect is the sum of indirect and direct effects. The simple correlations (last column of Table 5) include both the direct and indirect influences on J_R as well as spurious effects attributed to common causes.

The indirect and direct effects of some parameters add to produce a stronger total effect (N, V, IMF B_z, VLF, and ULF—Figure 5). With others, direct and indirect effects oppose each other (Dst and AE). As the model is constructed, the indirect effect of both VLF and ULF is due solely to their influence on J_S. Dst and AE act indirectly through VLF, ULF, and J_S, while N, V, and IMF B_z act indirectly through all the other parameters.

3.2. Prediction and Model Validation

We used the unstandardized regression coefficients to predict observations for each year. A nowcast model gives only a moderate correlation between predicted and observed J_R (range: 0.21–0.58; average: 0.35; Table 6). A model using predictors from the previous day gives similar correlations (0.22–0.64; average 0.39). Adding the previous day's flux to this Lag 1 model improves the correlation (0.71–0.89; average = 0.78). Correlations are lower when predictors (including previous J_R) are measured 3 days prior (Lag 3 model: 0.37–0.73, average = 0.51). A scatterplot of observed flux values from 1998 versus those predicted by the 1 day lag model (including 1 day lagged J_R) is given in Figure 6. Regression coefficients were produced from all data but 1998 and then used to calculate predicted flux values from the 1998 observed independent variables.

A time plot of these observed and predicted values shows how well predictions track observed flux levels during the third quarter of 1998 (Figure 7). The observed values (solid line) are well predicted by the 1 day lag model that includes lagged flux (dashed line). The 1 day lag model without flux underestimates the height of some peaks and overestimates others (dotted line). This is likely the cause of the lower correlation seen in the model validations. However, both models are able to predict increases, and a close inspection of each peak reveals that the model without lagged flux predicts flux increases slightly sooner than the model that includes lagged flux.

Table 5. Direct and Indirect Influences of 1 Day Lag Predictors[a]

	Effect on Flux (Direct Effect)	Dst	AE	VLF	ULF	Seed	Indirect Influence on Flux	Total Influence on Flux	Total Simple Correlation With Flux
N	−0.173	0.024	0.316	0.074	0.204	−0.150	−0.056	−0.229	−0.385
V	0.182	−0.528	0.732	0.137	0.454	0.128	0.123	0.305	0.422
B_z	−0.188	0.430	−0.576	0.103	−0.096	−0.16	−0.033	−0.221	−0.159
Dst	0.053			−0.030	−0.200	−0.183	−0.139	−0.086	−0.333
AE	−0.401		0.326		0.459	0.189	0.234	−0.167	0.239
VLF	0.014					0.077	0.032	0.046	0.149
ULF	0.163					0.333	0.141	0.304	0.340
Seed	0.422							0.422	0.477

[a]Relativistic electron flux persistence is not included in this model. Coefficients are from multiple regression analyses. Direct influences are from the multiple regression where relativistic electron flux is the dependent variable and predictor variables are lagged by 1 day. Path coefficients are from a series of multiple regressions with each predictor variable used as the dependent variable. The indirect influence is the sum of the product of all paths from a given predictor. Total influence is the sum of direct and indirect effects. Total correlation consists of both direct and indirect effects and spurious effects attributed to common causes.
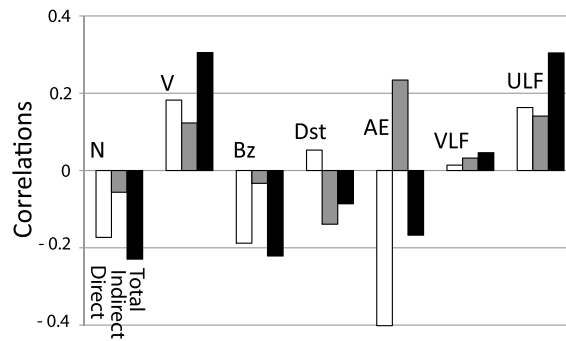
Figure 5. Direct (white bars), indirect (gray), and total (black) influence of each parameter on relativistic electron flux. Direct influence is the coefficients of the multiple regression where flux is the dependent variable. Other path coefficients (Table 5) are from regressions where each predictor variable is used as a dependent variable. Indirect influences are calculated by multiplying each coefficient in indirect paths from a variable to flux, then summing all such paths for that variable.

4. Discussion

In our previous study of relativistic electron flux following storms, ULF and seed electron flux were identified as the major influences in flux increases during recovery, with solar wind velocity and IMF B_z showing more modest correlations [*Simms et al.*, 2014]. In the current analysis of full years of data, including both quiet and storm times, seed electron flux correlates well on the same day (nowcast), but its influence drops off in the 1–3 day forecast models. Velocity and ULF activity are still associated with increased flux but only if measured 1–3 days before flux. They have little association in the nowcast model, where the major influences are negative effects of N and AE, and a positive influence of seed electron flux and Dst.

In our present study, we do not separate analyses or parameter measurements into periods of storm main phase or recovery or quiet periods. We attempt only to construct a model that describes the day to day dynamics of relativistic electrons, although mechanisms of electron loss and acceleration at different storm periods and during quiet periods may be controlled by different sets of parameters.

Some of our current correlations may also differ from those found in previous studies due to the multiple regression technique that we use. Multiple regression, by controlling for all variables simultaneously, gives a more accurate picture of each parameter's influence. If predictors are highly correlated, it is difficult to know, from simple correlation analysis, if a given parameter has any correlation with flux above and beyond the fact that it rises or falls in combination with more influential parameters. This is a particular problem in studying space weather phenomena where many possibly influential processes rise or fall simultaneously.

Our simple correlation analyses do give results similar to those found by previous studies. Seed electron flux (J_S), AE, solar wind velocity (V_x), and ULF wave power all have a positive influence on relativistic electron flux (J_R) (increases in the predictors are associated with increases in J_R), while number density (N) and Dst negatively impact flux (increases in the predictors are associated with decreases in J_R). The positive Dst effect (more negative Dst results in lower flux) on the same day is likely due to the temporary adiabatic decrease in flux seen during the main phase of storms [*Reeves et al.*, 2003; *Vassiliadis et al.*, 2005].

VLF wave activity and IMF B_z show more modest correlations (black bars of Figure 2). The low correlation of the ground VLF wave power may be because it is lowered by ionospheric attenuation in the summer months and may be measured at L shells where VLF has little influence on geostationary relativistic electron flux [*Smith et al.*, 2004b; *Thorne et al.*, 2013]. The lower influence of VLF measured on the same day relative to the influence at increasing lags may be due to the disruption of ducted propagation paths

Table 6. Correlations Between Observed Values From Each Year and Values Predicted From the Unstandardized Regression Coefficients of the Multiple Regression Models[a]

| Validation Year	Nowcast	Lag 1	Lag 1 With Previous Flux	Lag 3
1992	0.32	0.31	0.71	0.50
1994	0.51	0.60	0.85	0.69
1995	0.58	0.64	0.86	0.57
1996	0.47	0.56	0.89	0.73
1997	0.21	0.33	0.75	0.37
1998	0.27	0.28	0.77	0.47
1999	0.40	0.44	0.77	0.46
2000	0.28	0.22	0.72	0.37
2001	0.27	0.30	0.75	0.46
2002	0.22	0.23	0.76	0.46
Avg r	0.35	0.39	0.78	0.51

[a]Validation year is withheld from the regression analysis and subsequently used as the validation data set. In Lag 1 are values predicted from data 1 day prior to relativistic electron flux measurement. Lag 3 values are predicted from 3 days prior. Scatterplot of observed versus predicted values for validation year 1998 is in Figure 6.
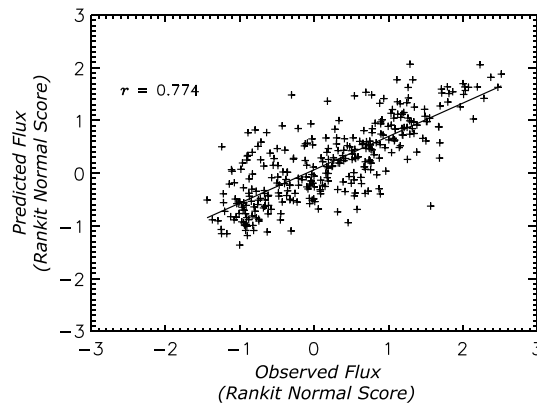
Figure 6. Validation of the regression model. Observed values of relativistic electron flux in 1998 versus values predicted by a multiple regression model using predictor values from 1 day previous (including the previous day's flux). Regression coefficients were produced from all data but 1998. Flux values are rankit normal scores. The correlation between observed and predicted values is 0.77. Correlations for other years are in Table 6.

from the source region to the lower altitudes (where the ground VLF is measured) during disturbed periods [*Smith et al.*, 2004a].

These simple correlations peak 1–3 days before the flux measurement. This has been reported before for ULF and VLF wave activity, and for solar wind velocity and number density [*Smith et al.*, 2004b; *Potapov et al.*, 2012, 2014; *Borovsky and Denton*, 2014]. We have found this lag in correlation to hold true for other variables as well (*AE*, seed electron flux, and *Dst*).

The strongest simple correlation is the 1 day lag of relativistic electron flux itself, confirming previous findings [*Ukhorskiy et al.*, 2004; *Sakaguchi et al.*, 2015]. In contrast, in storm-only models [*Simms et al.*, 2014], flux before a storm shows only modest predictive ability. Following storms, flux levels are more dependent on other parameters such as ULF wave activity, solar wind velocity, and main phase seed electron population. The stronger association between flux and its previous level in the all year models presented in our current study is due to the fact that flux changes little from day to day. A reasonably good prediction on most days can be made solely by predicting the next day's flux from the current day's. It takes many days or even weeks for the flux increases following a storm to return to quiet levels. Thus, the flux on 1 day following a storm will be similar to that on other days following that storm. The large stretches of quiet days with low flux levels that show little day to day variation would also give a strong correlation between flux on 1 day and flux on the next. This preponderance of days in the data set which there is little change explains the high predictive ability of the previous day's flux. However, a simple model such as this, while it would give high predictive ability, would miss the sudden changes that are of most interest. Persistence is also the least valuable factor in testing mechanisms of electron flux increases. The addition of other variables to the model via multiple regression not only improves the predictive ability but also gives insight into the mechanisms of electron acceleration which the simple measure of persistence does not. However, given the high correlations between predictor variables and previous flux, as well as the autocorrelation of the flux, previous day's flux must be added to the model as a covariate to clearly establish the role of other predictors.

Similarly, individual correlations of each variable with flux that do not account for other variables also run the risk of giving a skewed interpretation of the flux-predictor relationships [*Simms et al.*, 2010, 2014; *Potapov et al.*, 2012, 2014]. For example, a simple correlation between *Dst* and flux may not mean that changes in *Dst*
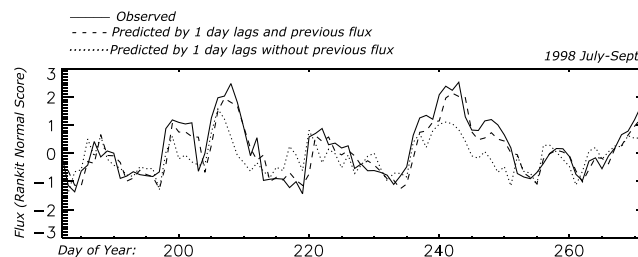
Figure 7. Timeplot of 1998 (third quarter) observed flux (solid line) versus that predicted by the 1 day lagged model with previous flux (dashed line) and by the 1 day lagged model without previous flux (dotted line). The addition of previous flux as a predictor improves the fit of the peak heights, but the model without previous flux better predicts the onset of a flux increase event. Flux values are rankit normal scores.

act to change flux levels. Other variables that occur along with *Dst* fluctuations and storms in general, such as ULF and VLF wave power, may be the drivers responsible for flux changes. *Dst* drops may only appear to be influential in simple correlations because these drops are associated with the wave power changes.

These complicated relationships explain why an attempt to build a multiple regression model using the most correlated lag of each predictor from the simple correlations does

not result in a better model than using the 1 day lags for each predictor. Although simple correlations for variables such as ULF or VLF peak at a 3 day lag, this does not mean that using the 3 day lag will result in ULF or VLF showing a greater influence in the regression model when all variables are analyzed together. The partial correlation analyses of Figure 2 point to this conclusion as well. Many of the variables, while showing a simple correlation peak at a 3 day lag, show a higher partial correlation at a 1 day lag.

Simultaneous testing of many variables in the multiple regression analyses we have performed can account for these intercorrelations and provide a firmer basis for deciding which variables may be responsible for flux changes.

4.1. Mechanisms Directly Driving Relativistic Electron Flux Increases

Fluxes of relativistic electrons in the magnetosphere are the result of a delicate balance between loss and acceleration. Only about half of storms increase flux, another quarter result in decreased flux, and the remainder show little change [*Reeves et al.*, 2003]. The first response to a storm is the net loss of relativistic electrons from the outer zone, while subsequent substorm activity in the recovery phase can lead to the net increases [*Li et al.*, 2009; *Meredith et al.*, 2002]. Direct electron injections from the plasma sheet due to enhanced convection can account for increases of the storm time energetic electrons ($E < 100$ keV) but cannot explain the rapid appearance of higher-energy electrons [*Liu et al.*, 2003; *Miyoshi et al.*, 2006; *Thorne et al.*, 2007]. An important aspect of high-energy electron dynamics is the availability of seed electrons that can be accelerated to high energies. Many studies show that electrons injected during storm main phase can be accelerated to subrelativistic energies ($100 < E < 500$ keV) and become "seeds" of the outer zone relativistic electrons ($E > 0.5$ MeV) [*Baker et al.*, 1998b; *Obara et al.*, 2000]. It has been suggested that Pi1 emissions are indicators of the midenergy electron interaction with the ionosphere that results in this necessary population of seed electrons [*Degtyarev et al.*, 2009, 2010]. This pool of seed electrons need not be large, as the energy spectrum of magnetospheric electrons is very steep. To produce the observed fluxes of relativistic electrons, only a small fraction of the seed electrons must be accelerated.

Other mechanisms have also been proposed to explain increases in relativistic electron flux. These include both proximal mechanisms such as acceleration by wave activity or substorms and more distal causes such as increased geomagnetic activity due to energy arriving in the solar wind.

ULF wave activity is often considered to be a possible driver of electron acceleration. The models proposed include enhanced radial diffusion by ULF waves [*Elkington et al.*, 1999; *Green and Kivelson,* 2004] which may take days to produce a significant increase in flux levels [*Liu et al.*, 1999], as well as models that depend on fast mode compressional ULF waves which could accelerate a large number of electrons over time scales from a few hours to several days, depending on amplitude [*Summers and Ma*, 2000b].

Using multiple regression, we find the strongest ULF-flux association occurs 3 days before the measured flux, confirming the previous findings of the simple correlations [*Potapov et al.*, 2012, 2014]. *Romanova et al.* [2007] discovered that a cumulative ULF index (integrated over 2–3 days prior to the flux measurement) was found to better correlate with relativistic electron flux than the original hourly ULF index as it evens out bursts of wave activity. The 24 h average of the ULF index we use in our present study is similar to the cumulative ULF index used by *Romanova et al.* [2007]. We chose not to use the cumulative ULF index in order to average all parameters over the same 24 h. Also, by using an average that included fewer days, we were able to more precisely pinpoint the timeframe of action. These findings that ULF activity acts over a period of days suggest that ULF waves accelerate electrons via a diffusion process which acts cumulatively [*Romanova et al.*, 2007; *Ozeke et al.*, 2012; *Potapov et al.*, 2014].

VLF chorus activity has also been shown to accelerate electrons and has been used in numerous models [*Horne and Thorne*, 1998; *Summers and Ma*, 2000a; *Albert et al.*, 2009; *Tu et al.*, 2014]. Correlations between VLF activity and increased electron flux provide support for this idea [*Meredith et al.*, 2003a; *O'Brien et al.*, 2003; *Smith et al.*, 2004b; *Horne et al.*, 2005; *Miyoshi et al.*, 2013; *Thorne et al.*, 2013; *Li et al.*, 2014; *Su et al.*, 2014; *Turner et al.*, 2014; *Xiao et al.*, 2014]. As noted above for the simple correlation analysis, the VLF influence may not be as high in the nowcast model only because ducted propagation of the waves to the ground stations may be attenuated during storm periods [*Smith et al.*, 2004a].

In our multivariable analysis, VLF wave activity does show an association with increased relativistic electron flux in the days preceding, but its influence is less than that of ULF wave activity. It is unclear whether this

is the result of an actual difference in the effect of VLF waves versus ULF waves or if the observed difference is due to measurement effects. In our previous multiple regression study of flux following storms, we found little effect of the ground VLF measurement [*Simms et al.*, 2014]; however, in a second study focusing on the reasons for this lack of influence, we found that the ground VLF correlation could be improved by limiting VLF observations to the dawn period (06:00–09:00 MLT at Halley) when electron acceleration due to chorus VLF waves is thought to dominate [*Simms et al.*, 2015]. We use this dawn period ground VLF measure in this paper as well; however, there may still be difficulties with solar illumination of the ionosphere in the summer months reducing observed VLF wave amplitude [*Smith et al.*, 2010].

A lower effect of VLF activity at geosynchronous orbit has been noted before, although in a study where VLF power was measured by the proxy of microburst frequency and not directly [*O'Brien et al.*, 2003]. As explained in their study, the use of microbursts as a proxy will tend to underestimate VLF activity at low levels of flux. This may have the effect of increasing the apparent correlation of VLF activity, if high levels of VLF activity are occurring during low flux levels when the VLF activity cannot be observed. Thus, in their study, the correlation of VLF activity with flux may be even lower than reported.

However, although there are many examples of satellite observations showing VLF waves leading directly to relativistic electron flux enhancement [*Horne et al.*, 2005; *Thorne et al.*, 2013; *Li et al.*, 2014; *Su et al.*, 2014; *Turner et al.*, 2014; *Xiao et al.*, 2014], observations and theory suggest that VLF waves may act to precipitate electrons into the loss cone as well, depending on the pitch angle and energy of these electrons [*Horne and Thorne*, 2003; *Lorentzen et al.*, 2001; *O'Brien et al.*, 2004; *Summers et al.*, 2007; *Thorne et al.*, 2005; *Saito et al.*, 2012; *Neal et al.*, 2015]. Thus, the overall VLF wave effect that we see may include both acceleration and precipitation, resulting in VLF activity having a negligible net influence on the level of flux of relativistic electrons.

O'Brien et al. [2003] also found that at $L \sim 4.5$, ULF wave activity and a proxy for VLF activity combined to produce higher relativistic flux than either could alone. We have found this to be the case at geosynchronous orbit as well. VLF and ULF wave activity act synergistically and not just additively, as seen in the significant interaction term of the multiple regressions. At higher levels of VLF, ULF has more effect and vice versa, and their combined contribution is more than the sum of their individual contributions.

This agrees with the model of *Li et al.* [2005] who found that the combined effect of electron acceleration (with the spread of the distribution function toward high-energy tail) by VLF and ULF wave activity in the same region is greater than a simple superposition of the two effects and the action of the VLF waves will often be dependent on the presence of ULF waves. They numerically solved a quasi-linear diffusion equation for ULF fast mode compressional turbulence with power law scale distribution and the whistler-mode turbulence with a Gaussian frequency distribution. While substorm injected energetic electrons can be regarded as seed particles that can be accelerated by whistler-mode turbulence, compressional ULF waves can accelerate both energetic electrons and background hot electrons. Thus, electrons must be first accelerated from a lower energy to several hundred of keV by the action of ULF waves. After this, whistler waves accelerate electrons to relativistic energies. This may be an important factor to incorporate into future models of flux enhancements. However, the fast mode in the Pc5 band is a rather rare phenomenon. Intense compressional waves during recovery (storm-related Pc5 pulsations) are usually attributed to poloidal Alfven waves instead [*Tan et al.*, 2011]. Therefore, this model may not be adequate to explain all instances of VLF-ULF interactive effects. Nonetheless, the idea of combined ULF-VLF acceleration is promising. One possible scenario is that ULF wave activity provides radial particle transport and that these particles are locally accelerated by VLF turbulence.

4.2. Distal Versus Proximal Influences

A further refinement to multiple regression is path analysis, in which presumed causal connections can be tested. The proximal variables discussed above are postulated to act directly on flux. The more distal factors of the solar wind and IMF are thought to control relativistic electron flux indirectly due to their ability to increase the wave and substorm activity which are the direct drivers [*Mathie and Mann*, 2000; *Mann et al.*, 2013]. A complicated model results where energy input from the solar wind and IMF causes an increase in the ring current (measured as a decrease in *Dst*, perhaps to storm levels), an increase in substorm activity (measured by *AE*), and increased wave activity in the ULF and VLF ranges. The geomagnetic disturbance

may further increase wave activity, as well as increase the seed population of electrons. The wave activity is then thought to act to accelerate the lower energy electrons to relativistic energies. This model of action is laid out in our path analysis. The path analysis is itself only a correlation analysis, but by distinguishing between proximal and distal factors, it allows for testing of the presumed causal connections [*Loehlin*, 1991]. We can test the direct influence of distal factors (solar wind and IMF factors) on relativistic electron flux as well as their influence on intermediary parameters that subsequently influence flux.

The direct effects of 1 day lagged number density, velocity, *Dst*, and substorms (*AE*) are of lower magnitude than their indirect effects through other variables (Figures 4 and 5). That there is any direct effect at all from these parameters suggests that there are additional mechanisms than just the indirect effects mediated through wave activity and seed electron flux. The direct positive effect of *Dst* on relativistic electron flux when other parameters are held constant is one obvious example. This is theorized to be the result of conservation of adiabatic invariants, causing electrons to move outward in response to the decreased magnetic field during storm main phase [*Kim and Chan*, 1997; *Li et al.*, 1997]. However, despite this positive correlation (when *Dst* is most negative, relativistic electron flux decreases), the overall correlation of *Dst* with flux is negative because the greater magnitude of the indirect effects of *Dst* mediated through wave activity and seed electron flux. This supports the hypothesis that ring current ions drive poloidal mode ULF wave activity which in turn leads to increased J_R [*Ozeke and Mann*, 2008].

Substorm activity is postulated to trigger higher flux [*Meredith et al.*, 2002; *O'Brien et al.*, 2003], possibly due to substorm dipolarization inducing electric fields that accelerate electrons in the geomagnetic tail which are then transported closer to the Earth by radial diffusion [*Kim et al.*, 2000]. This hypothesis is supported by the positive simple correlation we and other studies find between the *AE* measure of substorm activity and flux increases [*Kim et al.*, 2015; *Rodger et al.*, 2016]. *Rodger et al.* [2016] also find a much greater effectiveness of repetitive substorms which occur within 82 min of each other. Steady magnetospheric convection (SMC) of periods lasting longer than 90 min also produce higher levels of relativistic electrons following storms [*Kissinger et al.*, 2014]. SMC intervals show longer lasting and greater magnetospheric and ionospheric convection than an individual substorm recovery phase and are defined as periods with steady *AL* and enhancement of both *AL* and *AU* [*Kissinger et al.*, 2012]. The daily average *AE* index that we use encompasses single substorms, repetitive substorms, and SMC intervals. It is unclear if a statistic that differentiated between these periods would lead to different conclusions about the influence of single substorms versus more prolonged activity, but we plan to incorporate a more refined measure in future work.

However, the daily average of *AE* (our substorm measure) has a positive influence on seed electron flux and ULF and VLF wave activity, which themselves then positively impact flux levels. This confirms previous observations that substorms enhance VLF wave activity [*Meredith et al.*, 2002, 2003a; *Rodger et al.*, 2016], ULF wave activity [*Kozyreva and Kleimenova*, 2008; *Rae et al.*, 2011; *Simms et al.*, 2014] and seed electron flux [*Li et al.*, 2009]. While substorms may therefore show an overall positive influence in a simple correlation, this may be due only to substorms indirectly influencing J_R by enhancing wave activity and J_S. When wave activity and J_S are accounted for in multiple regression, the only effect of substorms left to measure may be their direct negative influence.

As substorm influences might only be expected to occur on the nightside, this may further explain why the ULF and VLF wave influences do not occur immediately. Our reduced models that sequentially add ULF or seed electrons show that once these parameters are included, *AE* shows no direct positive influence on flux (Table 4). The positive *AE* simple correlation with J_R, therefore, is only through its effects on ULF and seed electron enhancements. (Our measure of ULF, which emphasizes Pc5 pulsations, may not be the only ULF influence in this system. *Degtyarev et al.* [2009] also found a correlation between Pi1 pulsations and increased J_R. This may be due to the correlation of J_S to Pi1 pulsations as the Pi1 pulsations are an indicator of injection of low-energy electrons into the ionosphere which may indicate the presence of seed electrons in the magnetosphere.)

Given this, it might be predicted that once other factors are accounted for, the direct effect of *AE* on relativistic electron flux would be negligible. Surprisingly though, the direct effect of *AE* is negative. We at first hypothesized that this might be the result of including all days in our models: both storm and nonstorm periods. In particular, the physical processes that drive electron acceleration or depletion may be different during the main phase of storms. However, preliminary analyses in which we removed main phase days from the data set still resulted in a negative effect of *AE*, so this did not appear to be a promising avenue to explore.

The negative AE effect may be an artifact of substorm influences on other relevant processes that are not included in our model. The most likely candidate is electromagnetic ion cyclotron (EMIC) waves that are postulated to be driven by substorm injection of hot ion populations [*Clausen et al.*, 2011]. EMIC waves (Pc1-Pc2 pulsations of 0.1–5 Hz) are thought to precipitate relativistic electrons [*Meredith et al.*, 2003b; *Jordanova et al.*, 2008; *Miyoshi et al.*, 2008; *Kersten et al.*, 2014; *Usanova et al.*, 2014; *Engebretson et al.*, 2015]. Thus, substorm activity (measured by the AE index) may be responsible both for increasing flux via increased ULF and VLF wave activity and seed electron flux, as well as decreasing it by generating EMIC waves. As we did not include EMIC wave activity in our model, its negative influence may appear as a strongly negative AE direct effect. Unfortunately, there is no EMIC wave database for this stretch of time. If possible, we intend to include this parameter in future work. However, AE may not be a good measure of substorm activity during storms as many types of nonsubstorm activity, such as steady magnetospheric convection and electrojet variations, may be included in the storm time AE measure (Kyle Murphy, personal communication, 2015). This may complicate the interpretation of the influence of the AE index in our data set that spans both storm and nonstorm conditions. A further problem is that the AE index is determined from activity at the same magnetometers that provide the ULF index data. Thus, the ULF index may already include the AE activity and thus the prediction of any acceleration due to substorm onset. This may explain why both indices are not needed in the models.

High number density at geosynchronous orbit has also been postulated to generate more EMIC waves [*Clausen et al.*, 2011]. Therefore, this might be the same mechanism that results in a negative direct effect of number density in our path analysis. As number density also positively impacts AE (with its direct negative effect on relativistic electron flux) and negatively affects seed electron flux, many of the paths from number density add together to give this parameter a strong negative effect overall. Its positive effects through increased ULF and VLF wave activity are of lesser impact.

Our path analysis model could be further elaborated in the future by including interactions between substorm injection of both "source" electrons with energies of tens of keV that may enhance VLF wave activity as well as the seed electrons in our current model that are thought to be accelerated up to relativistic speeds by VLF waves [*Thorne et al.*, 2013; *Jaynes et al.*, 2015].

4.3. Assessment of Model Predictions

The correlation between prediction and observation from full year regression models is somewhat higher than that found with models using only data from storm recovery periods. *Simms et al.* [2014] found an average correlation of 0.720 between model predictions and novel observations from storm recovery periods (range: 0.645–0.784). The all year predictions from the 1 day lagged predictors of the present study show an average 0.78 correlation with observations (range: 0.71–0.89). These models predict the expected highest daily values of electron fluxes at geosynchronous orbit surprisingly well, despite covering both quiet and disturbed time periods in which physical processes are expected to be quite different.

Previously published predictive models at geosynchronous orbit generated from single solar wind parameters have resulted in correlations with observations ranging from around 0.15 (with B_z south as the sole predictor) to 0.35 (with N as the predictor) to 0.55 (using velocity as the predictor). Predictions using geomagnetic indices such as Dst, AL, or AU result in correlations with observations of about 0.40 [*Vassiliadis et al.*, 2005]. Our multivariable models improve on this predictive ability.

In the all year models, the data-derived 1 day lag models gave the best correlation with observations from outside the data set used to derive the model. Nowcast and 3 day lag models were not as predictive. We compared two 1 day lag models, one with previous relativistic flux as one of the predictors and one without it. The correlation to novel observations was higher when previous flux was included as a predictor; however, this was only because this model predicted the peak flux levels better. The 1 day lag model without previous flux does not predict the actual height of a peak well but is slightly better at predicting the onset of the increases. If the goal of a prediction model is to predict the peak of the relativistic electron flux increase, then the model with lagged flux would be more useful, but if the timing of the rise is more important, then the model without lagged flux would be preferred.

5. Summary

We predict J_R, the daily maximum relativistic electron flux at geostationary orbit, with an empirical model obtained from multiple regression analysis. Multiple regression allows the incorporation of many correlated predictor variables, determining the influence of each parameter while holding the other predictor variables constant. The most explanatory variables are the previous day's solar wind number density and velocity, AE index, and ULF wave activity; however, the AE index, measuring substorm processes, shows a negative correlation with flux when other parameters are controlled. This may be due to the fact that substorms do not act directly on flux enhancements but rather provide the seed electrons and the energy that drives wave activity (both ULF and VLF) to accelerate electrons The remaining portion of the substorm effect may be mediated through other unmeasured parameters such as EMIC waves that act to precipitate electrons. VLF waves measured at a ground station show a lower, but still significant, influence. ULF and VLF waves act synergistically on J_R, with each increasing the influence of the other.

Due to high persistence of relativistic electrons in the radiation belt, the addition of the previous day's J_R as a predictor improves the correlation between predicted observations and observations from an independent set of data. However, this improved correlation is apparently only due to a better prediction of the level of flux. Its addition to the model delays the anticipation of a flux event.

References

Albert, J. M., N. P. Meredith, and R. B. Horne (2009), Three-dimensional diffusion simulation of outer radiation belt electrons during the 9 October 1990 magnetic storm, *J. Geophys. Res.*, *114*, A09214, doi:10.1029/2009JA014336.

Baker, D. N., R. D. Belian, P. R. Higbie, R. W. Klebesadel, and J. B. Blake (1987), Deep dielectric charging effects due to high energy electrons in the Earth's outer magnetosphere, *J. Electrost.*, *20*, 3–19.

Baker, D. N., J. H. Allen, S. G. Kanekal, and G. D. Reeves (1998a), Disturbed space environment may have been related to pager satellite failure, *Eos Trans. AGU*, *79*, 477, doi:10.1029/98EO00359.

Baker, D. N., T. Pulkkinen, X. Li, S. G. Kanekal, J. B. Blake, R. S. Selesnick, M. G. Henderson, G. D. Reeves, H. E. Spence, and G. Rostoker (1998b), Coronal mass ejections, magnetic clouds, and relativistic magnetospheric electron event: ISTP, *J. Geophys. Res.*, *103*, 17,279–17,291, doi:10.1029/97JA03329.

Balikhin, M. A., R. J. Boynton, S. N. Walker, J. E. Borovsky, S. A. Billings, and H. L. Wei (2011), Using the NARMAX approach to model the evolution of energetic electrons fluxes at geostationary orbit, *Geophys. Res. Lett.*, *38*, L18105, doi:10.1029/2011GL048980.

Borovsky, J. E., and M. H. Denton (2014), Exploring the cross correlations and autocorrelations of the ULF indices and incorporating the ULF indices into the systems science of the solar wind-driven magnetosphere, *J. Geophys. Res. Space Physics*, *119*, 4307–4334, doi:10.1002/2014JA019876.

Clausen, L. B. N., J. B. H. Baker, J. M. Ruohoniemi, and H. J. Singer (2011), EMIC waves observed at geosynchronous orbit during solar minimum: Statistics and excitation, *J. Geophys. Res.*, *116*, A10205, doi:10.1029/2011JA016823.

Degtyarev, V. I., I. P. Kharchenko, A. S. Potapov, B. Tsegmed, and S. E. Chudnenko (2009), Qualitative estimation of magnetic storm efficiency in producing relativistic electron flux in the Earth's outer radiation belt using geomagnetic pulsations data, *Adv. Space Res.*, *43*, 829–836, doi:10.1016/j.asr.2008.07.004.

Degtyarev, V. I., I. P. Kharchenko, A. S. Potapov, B. Tsegmed, and S. E. Chudnenko (2010), The relation between geomagnetic pulsations and an increase in the fluxes of geosynchronous relativistic electrons during geomagnetic storms, *Geomagn. Aeron.*, *50*(7), 885–893.

Elkington, S. R., M. K. Hudson, and A. A. Chan (1999), Acceleration of relativistic electrons via drift-resonance interaction with toroidal-mode Pc5 oscillations, *Geophys. Res. Lett.*, *26*, 3273–3276, doi:10.1029/1999GL003659.

Engebretson, M. J., et al. (2015), Van Allen probes, NOAA, GOES, and ground observations of an intense EMIC wave event extending over 12 h in magnetic local time, *J. Geophys. Res. Space Physics*, *120*, 5465–5488, doi:10.1002/2015JA021227.

Golden, D. I., M. Spasojevic, W. Li, and Y. Nishimura (2012), Statistical modeling of plasmaspheric hiss amplitude using solar wind measurements and geomagnetic indices, *Geophys. Res. Lett.*, *39*, L06103, doi:10.1029/2012GL051185.

Green, J. C., and M. G. Kivelson (2004), Relativistic electrons in the outer radiation belt: Differentiating between acceleration mechanisms, *J. Geophys. Res.*, *109*, A03213, doi:10.1029/2003JA010153.

Horne, R. B., and R. M. Thorne (1998), Potential waves for relativistic electron scattering and stochastic acceleration during magnetic storms, *Geophys. Res. Lett.*, *25*, 3011–3014, doi:10.1029/98GL01002.

Horne, R. B., and R. M. Thorne (2003), Relativistic electron acceleration and precipitation during resonant interactions with whistler-mode chorus, *Geophys. Res. Lett.*, *30*(10), 1527, doi:10.1029/2003GL016973.

Horne, R. B., R. M. Thorne, S. A. Glauert, J. M. Albert, N. P. Meredith, and R. R. Anderson (2005), Timescale for radiation belt electron acceleration by whistler mode chorus waves, *J. Geophys. Res.*, *110*, A03225, doi:10.1029/2004JA010811.

Jaynes, A. N., et al. (2015), Source and seed populations for relativistic electrons: Their roles in radiation belt changes, *J. Geophys. Res. Space Physics*, *120*, 7240–7254, doi:10.1002/2015JA021234.

Jordanova, V. K., J. Albert, and Y. Miyoshi (2008), Relativistic electron precipitation by EMIC waves from self-consistent global simulations, *J. Geophys. Res.*, *113*, A00A10, doi:10.1029/2008JA013239.

Kellerman, A. C., and Y. Y. Shprits (2012), On the influence of solar wind conditions on the outer-electron radiation belt, *J. Geophys. Res.*, *117*, A05217, doi:10.1029/2011JA017253.

Kersten, T., R. B. Horne, S. A. Glauert, N. P. Meredith, B. J. Fraser, and R. S. Grew (2014), Electron losses from the radiation belts caused by EMIC waves, *J. Geophys. Res. Space Physics*, *119*, 8820–8837, doi:10.1002/2014JA020366.

Kim, H.-J., and A. A. Chan (1997), Fully adiabatic changes in storm time relativistic electron fluxes, *J. Geophys. Res.*, *102*, 22,107–22,116, doi:10.1029/97JA01814.

Kim, H.-J., A. A. Chan, R. A. Wolf, and J. Birn (2000), Can substorms produce relativistic outer belt electrons?, *J. Geophys. Res.*, *105*, 7721–7735, doi:10.1029/1999JA900465.

Kim, H.-J., L. Lyons, V. Pinto, C.-P. Wang, and K.-C. Kim (2015), Re-visit of relationship between geosynchronous relativistic electron enhancements and magnetic storms, *Geophys. Res. Lett.*, *42*, 6155–6161, doi:10.1002/2015GL065192.

Kissinger, J., R. L. McPherron, T.-S. Hsu, and V. Angelopoulos (2012), Diversion of plasma due to high pressure in the inner magnetosphere during steady magnetopheric convection, *J. Geophys. Res.*, *117*, A05206, doi:10.1029/2012JA017579.

Kissinger, J., L. Kepko, D. N. Baker, S. Kanekal, W. Li, R. L. McPherron, and V. Angelopous (2014), The importance of storm time steady magnetospheric convection in determining the final relativistic electron flux level, *J. Geophys. Res. Space Physics*, *119*, 7433–7443, doi:10.1002/2014JA019948.

Kozyreva, O., V. Pilipenko, M. J. Engebretson, K. Yumoto, J. Watermann, and N. Romanova (2007), In search of a new ULF wave index: Comparison of Pc5 power with dynamics of geostationary relativistic electrons, *Planet. Space Sci.*, *55*, 755–769.

Kozyreva, O. V., and N. G. Kleimenova (2008), Average ULF intensity level during strong geomagnetic storms, "Physics of Auroral Phenomena", in *Proc. XXXI Annual Seminar*, pp. 25–28, Kola Sci. Centre, Russian Acad. of Sci., Apatity, Russia.

Lanzerotti, L. J. (2001), Space weather effects on communications, in *Space Storms and Space Weather Hazards*, *NATO Sci. Ser. II: Math., Phys. and Chem.*, vol. 38, edited by I. Daglis, 313 pp., Kluwer Acad., Dordrecht, Netherlands.

Li, L., J. B. Cao, and G. C. Zhou (2005), Combined acceleration of electrons by whistler-mode and compressional ULF turbulences near the geosynchronous orbit, *J. Geophys. Res.*, *110*, A03203, doi:10.1029/2004JA010628.

Li, L. Y., J. B. Cao, G. C. Zhou, and X. Li (2009), Statistical roles of storms and substorms in changing the entire outer zone relativistic electron population, *J. Geophys. Res.*, *114*, A12214, doi:10.1029/2009JA01433.

Li, W., et al. (2014), Radiation belt electron acceleration by chorus waves during the 17 March 2013 storm, *J. Geophys. Res. Space Physics*, *119*, 4681–4693, doi:10.1002/2014JA019945.

Li, X., D. N. Baker, M. Temerin, T. E. Cayton, G. D. Reeves, R. A. Christensen, J. B. Blake, M. D. Looper, R. Nakamura, and S. G. Kanekal (1997), Multi-satellite observations of the outer zone electron variation during the 3–4 November 1993 magnetic storm, *J. Geophys. Res.*, *102*, 14,123–14,140, doi:10.1029/97JA01101.

Li, X., M. Temerin, D. N. Baker, and G. D. Reeves (2011), Behavior of MeV electrons at geosynchronous orbit during last two solar cycles, *J. Geophys. Res.*, *116*, A11207, doi:10.1029/2011JA016934.

Liu, S., M. W. Chen, L. R. Lyons, H. Korth, J. M. Albert, J. L. Roeder, P. C. Anderson, and M. F. Thomsen (2003), Contribution of convective transport to stormtime ring current electron injection, *J. Geophys. Res.*, *108*(A10), 1372, doi:10.1029/2003JA010004.

Liu, W. W., G. Rostoker, and D. N. Baker (1999), Internal acceleration of relativistic electrons by large-amplitude ULF pulsations, *J. Geophys. Res.*, *104*, 17,391–17,407, doi:10.1029/1999JA900168.

Loehlin, J. (1991), *Latent Variable Models: An Introduction to Factor, Path and Structural Analysis*, Lawrence Erlbaum, Hillsdale, N. J.

Lorentzen, K. R., J. B. Blake, U. S. Inan, and J. Bortnik (2001), Observations of relativistic electron microbursts in association with VLF chorus, *J. Geophys. Res.*, *106*, 6017–6027.

Lyatsky, W., and G. V. Khazanov (2008), Effect of geomagnetic disturbances and solar wind density on relativistic electrons at geostationary orbit, *J. Geophys. Res.*, *113*, A08224, doi:10.1029/2008JA013048.

Lyons, L. R., D.-Y. Lee, R. M. Thorne, R. B. Horne, and A. J. Smith (2005), Solar wind-magnetosphere coupling leading to relativistic electron energization during high-speed streams, *J. Geophys. Res.*, *110*, A11202, doi:10.1029/2005JA011254.

Mann, I. R., K. R. Murphy, L. G. Ozeke, I. J. Rae, D. K. Milling, A. Kale, and R. Honary (2013), The role of ultralow frequency waves in radiation belt dynamics, in *Dynamics of the Earth's Radiation Belts and Inner Magnetosphere*, *Geophys. Monogr. Ser.*, vol. 199, edited by D. Summers et al., pp. 69–92, AGU, Washington, D. C., doi:10.1029/GM199.

Mathie, R. A., and I. R. Mann (2000), A correlation between extended intervals of ULF wave power and storm-time geosynchronous electron flux enhancements, *Geophys. Res. Lett.*, *27*, 3261–3264, doi:10.1029/2000GL003822.

Meredith, N. P., R. B. Horne, R. H. A. Iles, R. M. Thorne, D. Heynderickx, and R. R. Anderson (2002), Outer zone relativistic electron acceleration associated with substorm-enhanced whistler mode chorus, *J. Geophys. Res.*, *107*(A7), 1144, doi:10.1029/2001JA900146.

Meredith, N. P., M. Cain, R. B. Horne, R. M. Thorne, D. Summers, and R. R. Anderson (2003a), Evidence for chorus-driven electron acceleration to relativistic energies from a survey of geomagnetically disturbed periods, *J. Geophys. Res.*, *108*(A6), 1248, doi:10.1029/2002JA009764.

Meredith, N. P., R. M. Thorne, R. B. Horne, D. Summers, B. J. Fraser, and R. R. Anderson (2003b), Statistical analysis of relativistic electron energies for cyclotron resonance with EMIC waves observed on CRRES, *J. Geophys. Res.*, *108*(A6), 1250, doi:10.1029/2002JA009700.

Miyoshi, Y., K. Sakaguchi, K. Shiokawa, D. Evans, J. Albert, M. Connors, and V. Jordanova (2008), Precipitation of radiation belt electrons by EMIC waves, observed from ground and space, *Geophys. Res. Lett.*, *35*, L23101, doi:10.1029/2008GL035727.

Miyoshi, Y., R. Kataoka, Y. Kasahara, A. Kumamoto, T. Nagai, and M. F. Thomsen (2013), High-speed solar wind with southward interplanetary magnetic field causes relativistic electron flux enhancement of the outer radiation belt via enhanced condition of whistler waves, *Geophys. Res. Lett.*, *40*, 4520–4525, doi:10.1002/grl.50916.

Miyoshi, Y. S., V. K. Jordanova, A. Morioka, M. F. Thomsen, G. D. Reeves, D. S. Evans, and J. C. Green (2006), Observations and modeling of energetic electron dynamics during the October 2001 storm, *J. Geophys. Res.*, *111*, A11S02, doi:10.1029/2005JA011351.

Neal, J. J., C. J. Rodger, M. A. Clilverd, N. R. Thomson, T. Raita, and T. Ulich (2015), Long-term determination of energetic electron precipitation into the atmosphere from AARDDVARK subionospheric VLF observations, *J. Geophys. Res. Space Physics*, *120*, 2194–2211, doi:10.1002/2014JA020689.

Neter, J., W. Wasserman, and M. H. Kutner (1985), *Applied Linear Statistical Models*, Richard D. Irwin, Inc., Homewood, Ill.

Obara, T., T. Nagatsuma, M. Den, Y. Miyoshi, and A. Morioka (2000), Main phase creation of "seed" electrons in the outer radiation belt, *Earth Planets Space*, *52*, 41–47.

O'Brien, T. P., and R. L. McPherron (2003), An empirical dynamic equation for energetic electrons at geosynchronous orbit, *J. Geophys. Res.*, *108*(A3), 1137, doi:10.1029/2002JA009324.

O'Brien, T. P., K. R. Lorentzen, I. R. Mann, N. P. Meredith, J. B. Blake, J. F. Fennell, M. D. Looper, D. K. Milling, and R. R. Anderson (2003), Energization of relativistic electrons in the presence of ULF power and MeV microbursts: Evidence for dual ULF and VLF acceleration, *J. Geophys. Res.*, *108*(A8), 1329, doi:10.1029/2002JA009784.

O'Brien, T. P., M. D. Looper, and J. B. Blake (2004), Quantification of relativistic electron microburst losses during the GEM storms, *Geophys. Res. Lett.*, *31*, L04802, doi:10.1029/2003GL018621.

Ozeke, L. G., and I. R. Mann (2008), Energization of radiation belt electrons by ring current ion driven ULF waves, *J. Geophys. Res.*, *113*, A02201, doi:10.1029/2007JA012468.

Ozeke, L. G., I. R. Mann, K. R. Murphy, I. J. Rae, D. K. Milling, S. R. Elkington, A. A. Chan, and H. J. Singer (2012), ULF wave derived radiation belt radial diffusion coefficients, *J. Geophys. Res.*, *117*, A04222, doi:10.1029/2011JA017463.

Pilipenko, V., N. Yagova, N. Romanova, and J. Allen (2006), Statistical relationships between satellite anomalies at geostationary orbit and high-energy particles, *Adv. Space Res.*, *37*, 1192–1205.

Potapov, A. S., B. Tsegmed, and L. V. Ryzhakova (2012), Relationship between the fluxes of relativistic electrons at geosynchronous orbit and the level of ULF activity on the Earth's surface and in the solar wind during the 23rd solar activity cycle, *Cosmic Res.*, *50*, 124–140.

Potapov, A. S., B. Tsegmed, and L. V. Ryzhakova (2014), Solar cycle variation of "killer" electrons at geosynchronous orbit and electron flux correlation with the solar wind parameters and ULF waves intensity, *Acta Astronaut.*, *93*, 55–63.

Rae, I. J., K. R. Murphy, C. E. J. Watt, and I. R. Mann (2011), On the nature of ULF wave power during nightside auroral activations and substorms: 2. Temporal evolution, *J. Geophys. Res.*, *116*, A00I22, doi:10.1029/2010JA015762.

Reeves, G. D., K. L. McAdams, R. H. W. Friedel, and T. P. O'Brien (2003), Acceleration and loss of relativistic electrons during geomagnetic storms, *Geophys. Res. Lett.*, *30*(10), 1529, doi:10.1029/2002GL016513.

Rodger, C. J., K. Cresswell-Moorcock, and M. A. Clilverd (2016), Nature's Grand Experiment: Linkage between magnetospheric convection and the radiation belts, *J. Geophys. Res. Space Physics*, *121*, 171–189, doi:10.1002/2015JA02153.

Romanova, N., V. Pilipenko, N. Crosby, and O. Khabarova (2007), ULF wave index and its possible applications in space physics, *Bulg. J. Phys.*, *34*, 136–148.

Saito, S., Y. Miyoshi, and K. Seki (2012), Relativistic electron microbursts associated with whistler chorus rising tone elements: GEMSIS-RBW simulations, *J. Geophys. Res.*, *117*, A10206, doi:10.1029/2012JA018020.

Sakaguchi, K., T. Nagatsuma, G. D. Reeves, and H. E. Spence (2015), Prediction of MeV electron fluxes throughout the outer radiation belt using multivariate autoregressive models, *Space Weather*, *13*, 853–867, doi:10.1002/2015SW001254.

Simms, L. E., V. A. Pilipenko, and M. J. Engebretson (2010), Determining the key drivers of magnetospheric Pc5 wave power, *J. Geophys. Res.*, *115*, A10241, doi:10.1029/2009JA015025.

Simms, L. E., M. J. Engebretson, A. J. Smith, M. Clilverd, V. A. Pilipenko, and G. D. Reeves (2014), Prediction of relativistic electron flux following storms at geostationary orbit: Multiple regression analysis, *J. Geophys. Res. Space Physics*, *119*, 7297–7318, doi:10.1002/2014JA019955.

Simms, L. E., V. A. Pilipenko, M. J. Engebretson, G. D. Reeves, A. J. Smith, and M. Clilverd (2015), Analysis of the effectiveness of ground-based VLF wave observations for predicting or nowcasting relativistic electron flux at geostationary orbit, *J. Geophys. Res. Space Physics*, *120*, 2052–2060, doi:10.1002/2014JA020337.

Smith, A. J. (1995), VELOX: A new VLF/ELF receiver in Antarctica for the Global Geospace Science mission, *J. Atmos. Terr. Phys.*, *57*(5), 507–524.

Smith, A. J., R. B. Horne, and N. P. Meredith (2004a), Ground observations of chorus following geomagnetic storms, *J. Geophys. Res.*, *109*, A02205, doi:10.1029/2003JA010204.

Smith, A. J., N. P. Meredith, and T. P. O'Brien (2004b), Differences in ground-observed chorus in geomagnetic storms with and without enhanced relativistic electron fluxes, *J. Geophys. Res.*, *109*, A11204, doi:10.1029/2004JA010491.

Smith, A. J., R. B. Horne, and N. P. Meredith (2010), The statistics of natural ELF/VLF waves derived from a long continuous set of ground-based observations at high latitude, *J. Atmos. Terr. Phys.*, *72*, 463–475.

Sokal, R. R., and F. J. Rohlf (1995), *Biometry: The Principles and Practice of Statistics in Biological Research*, 3rd ed., 859 pp., W. H. Freeman, New York.

Su, Z., et al. (2014), Intense duskside lower band chorus waves observed by Van Allen Probes: Generation and potential acceleration effect on radiation belt electrons, *J. Geophys. Res. Space Physics*, *119*, 4266–4273, doi:10.1002/2014JA019919.

Summers, D., and C. Ma (2000a), A model for generating relativistic electrons in the Earth's inner magnetosphere based on gyroresonant wave-particle interactions, *J. Geophys. Res.*, *105*, 2625–2639, doi:10.1029/1999JA900444.

Summers, D., and C. Ma (2000b), Rapid acceleration of electrons in the magnetosphere by fast-mode MHD waves, *J. Geophys. Res.*, *105*, 15,887–15,895, doi:10.1029/1999JA000408.

Summers, D., B. Ni, and N. P. Meredith (2007), Timescales for radiation belt electron acceleration and loss due to resonant wave-particle interactions: 2. Evaluation for VLF chorus, ELF hiss, and electromagnetic ion cyclotron waves, *J. Geophys. Res.*, *112*, A04207, doi:10.1029/2006JA011993.

Tan, L. C., X. Shao, A. S. Sharma, and S. F. Fung (2011), Relativistic electron acceleration by compressional-mode ULF waves: Evidence from correlated Cluster, Los Alamos National Laboratory spacecraft, and ground-based magnetometer measurements, *J. Geophys. Res.*, *116*, A07226, doi:10.1029/2010JA016226.

Thorne, R. M., T. P. O'Brien, Y. Y. Shprits, D. Summers, and R. B. Horne (2005), Timescale for MeV electron microburst loss during geomagnetic storms, *J. Geophys. Res.*, *110*, A09202, doi:10.1029/2004JA010882.

Thorne, R. M., Y. Y. Shprits, N. P. Meredith, R. B. Horne, W. Li, and L. R. Lyons (2007), Refilling of the slot region between the inner and outer electron radiation belts during geomagnetic storms, *J. Geophys. Res.*, *112*, A06203, doi:10.1029/2006JA012176.

Thorne, R. M., et al. (2013), Rapid local acceleration of relativistic radiation-belt electrons by magnetospheric chorus, *Nature*, *504*, 411, doi:10.1038/nature12889.

Tu, W., G. S. Cunningham, Y. Chen, S. K. Morley, G. D. Reeves, J. B. Blake, D. N. Baker, and H. Spence (2014), Event-specific chorus wave and electron seed population models in DREAM3D using the Van Allen Probes, *Geophys. Res. Lett.*, *41*, 1359–1366, doi:10.1002/2013GL058819.

Turner, D. L., X. Li, E. Burin des Roziers, and S. Monk (2011), An improved forecast system for relativistic electrons at geosynchronous orbit, *Space Weather*, *9*, S06003, doi:10.1029/2010SW000647.

Turner, D. L., *et al.* (2014), Competing source and loss mechanisms due to wave-particle interactions in Earth's outer radiation belt during the 30 September to 3 October 2012 geomagnetic storm, *J. Geophys. Res. Space Physics*, *119*, 1960–1979, doi:10.1002/2014JA019770.

Ukhorskiy, A. Y., M. I. Sitnov, A. S. Sharma, B. J. Anderson, S. Ohtani, and A. T. Y. Lui (2004), Data-derived forecasting model for relativistic electron intensity at geosynchronous orbit, *Geophys. Res. Lett.*, *31*, L09806, doi:10.1029/2004GL019616.

Usanova, M. E., et al. (2014), Effect of EMIC waves on relativistic and ultrarelativistic electron populations: Ground-based and Van Allen Probes observations, *Geophys. Res. Lett.*, *41*, 1375–1381, doi:10.1002/2013GL059024.

Vassiliadis, D., S. F. Fung, and A. J. Klimas (2005), Solar, interplanetary, and magnetospheric parameters for the radiation belt energetic electron flux, *J. Geophys. Res.*, *110*, A04201, doi:10.1029/2004JA010443.

Xiao, F., et al. (2014), Chorus acceleration of radiation belt relativistic electrons during March 2013 geomagnetic storm, *J. Geophys. Res. Space Physics*, *119*, 3325–3332, doi:10.1002/2014JA019822.